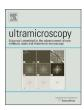
ELSEVIER

Contents lists available at ScienceDirect

Ultramicroscopy

journal homepage: www.elsevier.com/locate/ultramic



Phase measurement error in summation of electron holography series



Robert A. McLeod a,b,*, Michael Bergen b, Marek Malac b,a

- ^a Department of Physics, University of Alberta, Edmonton, AB, Canada T6G 2E1
- ^b National Institute for Nanotechnology, 11421 Saskatchewan Dr., Edmonton, AB, Canada T6G 2M9

ARTICLE INFO

Article history:
Received 26 March 2013
Received in revised form
2 March 2014
Accepted 9 March 2014
Available online 21 March 2014

Keywords:
Off-axis electron holography
Transmission electron microscope
Complex circular random variables
Phase error
Phase resolution
Random-walk
Quantitative electron microscopy
TEM optimization
Specimen drift
Microscope instabilities

ABSTRACT

Off-axis electron holography is a method for the transmission electron microscope (TEM) that measures the electric and magnetic properties of a specimen. The electrostatic and magnetic potentials modulate the electron wavefront phase. The error in measurement of the phase therefore determines the smallest observable changes in electric and magnetic properties. Here we explore the summation of a hologram series to reduce the phase error and thereby improve the sensitivity of electron holography. Summation of hologram series requires independent registration and correction of image drift and phase wavefront drift, the consequences of which are discussed. Optimization of the electro-optical configuration of the TEM for the double biprism configuration is examined. An analytical model of image and phase drift, composed of a combination of linear drift and Brownian random-walk, is derived and experimentally verified. The accuracy of image registration via cross-correlation and phase registration is characterized by simulated hologram series. The model of series summation errors allows the optimization of phase error as a function of exposure time and fringe carrier frequency for a target spatial resolution. An experimental example of hologram series summation is provided on WS2 fullerenes. A metric is provided to measure the object phase error from experimental results and compared to analytical predictions. The ultimate experimental object root-mean-square phase error is 0.006 rad $(2\pi/1050)$ at a spatial resolution less than 0.615 nm and a total exposure time of 900 s. The ultimate phase error in vacuum adjacent to the specimen is 0.0037 rad $(2\pi/1700)$. The analytical prediction of phase error differs with the experimental metrics by +7% inside the object and -5% in the vacuum, indicating that the model can provide reliable quantitative predictions.

Crown Copyright © 2014 Published by Elsevier B.V. All rights reserved.

1. Introduction

Off-axis electron holography (EH) in the transmission electron microscope (TEM) is a technique for the characterization of electrostatic and magnetic properties of a specimen [1,2]. A population of electrons, each being a wave-particle, has a distribution of amplitude and phase shift in both time and space. The electron is phase shifted by the electric and magnetic potentials integrated along its path [3], most principally that of the object/specimen, analogous to the index of refraction of a material phase shifting a photon.

An attractive strategy for improving the signal-to-noise ratio (SNR) of electron holograms is summation of a hologram series. Two approaches have been historically used, one based on the phase-shifting algorithm [4–8] and the other on alignment of conventionally reconstruction hologram series [8,9]. This paper

E-mail address: robbmcleod@gmail.com (R.A. McLeod).

takes the second approach, first demonstrated by Voelkl and Tang, whereby the image drift and phase wavefront drift are separately registered and corrected. Where the previous work demonstrated proof of principle on amorphous carbon, we have attempted to provide a rigorous model of the system, demonstrated it on a more typical specimen at high resolution, and demonstrated quantitative agreement between the model and experiment.

An image series can be used to break a long exposure into frames with the image drift for each frame corrected by cross correlation. In an electron hologram the strongest feature is the fringes of the interference pattern, which shift with drift of the electron phase. As a result, application of cross-correlation alignment cannot be applied to electron holograms directly to correct the image drift. Registration of the image and phase drift must be performed separately, which requires operating on the complex data of the reconstructed hologram. In this paper we provide methods to optimize the phase error of hologram series as a function of the targeted spatial resolution.

In Section 2, we introduce the dependence of phase error on spatial resolution and how to optimize the microscope column. In Section 3 we extend the optimization for a hologram series, taking

^{*} Corresponding author at: Department of Physics, 4-183 CCIS, University of Alberta, Edmonton, AB, Canada T6G 2E1. Tel.: $+1\,780\,641\,1667$; fax: $+1\,780\,641\,1601$.

into account image and wavefront phase drift. In Section 4 we provide examples of high-resolution hologram series results on a specimen of inorganic fullerene WS₂. In Section 4.2 we develop a metric to measure phase error experimentally and compare it to the estimates derived in Section 3. A description of the algorithm used to align and sum a hologram series is found in the online supplemental material.

2. Optimization of electro-optical configuration

In off-axis electron holography, the electron wavefront is split by an electrostatic biprism. The object wave (subscript 1) passes through the specimen, while the reference wave (subscript 2) passes through vacuum adjacent to the specimen. The two waves converge on a detector at semi-angle θ , forming an interference fringe pattern, or hologram. The interference pattern intensity, $\psi_{12}^2(\mathbf{r})$, as a function of position $\mathbf{r} = r_{\mathbf{x}}\hat{\mathbf{x}} + r_{\mathbf{y}}\hat{\mathbf{y}}$, is given by,

$$\psi_{12}^{2}(\mathbf{r}) = A_{1}^{2}(\mathbf{r}) + A_{2}^{2}(\mathbf{r}) + 2V(\mathbf{r}, q_{c}, \alpha_{o})A_{1}(\mathbf{r})A_{2}(\mathbf{r})\cos(2\pi\mathbf{q_{c}}\mathbf{r} + \phi_{1}(\mathbf{r}) - \phi_{2}(\mathbf{r}))$$
(1)

where A_1 and A_2 are the object and reference wave amplitude, respectively, ϕ_1 and ϕ_2 are the object and reference wave phase shift, respectively, $|\mathbf{q}_c| = 2 \sin{(\theta)}/\lambda$, is the carrier frequency of the fringe pattern, V is the holographic visibility (or fringe contrast) which depends on the illumination angle α_0 and the separation of virtual sources determined by q_c .

The path length, i.e. phase, difference between the reference and object waves measures both the electrostatic potential background of the object, and the electrostatic and magnetic potentials/fields [10–12]. As with all measurements, there is an associated error that limits the minimum variation in specimen thickness, compositional variation, and electric and magnetic field that may be measured [13]. The standard error of the phase has historically been expressed by the estimate of its variance [14–17],

$$\sigma_{\phi}^2(\mu, V) \propto 2/\mu V^2$$
 (2)

where, μ is the number of electrons per reconstructed pixel and V is the holographic visibility, which may be calculated by various means [18]. Typically in the digital reconstruction process the filtering that isolates the sideband changes the signal-to-noise characteristics of the hologram considerably, as discussed below, so that Eq. (2) is a proportion. It may be used as a figure of merit to compare vacuum holograms under different illumination conditions, for example.

Minimization of phase error requires maximization of both current density and holographic visibility. Holographic visibility is largely dependent on the high wavefront coherence which results from parallel, widely-spread illumination. However, the more widely spread the illumination, the lower the current density incident on the specimen. Long exposure times may be used to increase the electron dose, but image drift, shifts in specimen position, and phase drift, changes in the electron path-length, blur the hologram in space and phase. Thus it is necessary to optimize the electro-optical configuration [19].

The estimator of Eq. (2) is limited in that it does not relate the spatial resolution to the phase error, although the two are linked [20]. For example, an estimated phase error of 0.001 rad $(2\pi/6300)$ with a measured phase noise of 0.02 rad $(2\pi/300)$ has been demonstrated at 12 nm spatial resolution [21], compared to an estimated phase error of ~ 0.06 $(2\pi/100)$ at 0.1 nm spatial resolution [22]. Phase error is related to spatial resolution, both due to the optical-transfer function (OTF) of the TEM [23] and modulation-transfer function (MTF) of the detector [24,25]. The down-sampling of the detector from the holographic reconstruction process also has a major impact on the mean dose per pixel.

As we show in Section 3, the drift of the image and holographic fringes also affects the phase error, especially for prolonged exposures at high spatial resolutions.

Reconstruction of electron holograms is typically done using the Fourier method [2,20]. In Fourier-space, a hologram consists of a central band at zero frequency (i.e. the autocorrelation) and two sidebands, one at the spatial frequency of the fringe pattern and the other at its complex conjugate. The phase shift is encoded in the positions of the fringe pattern, therefore reconstruction of the complex (amplitude and phase) electron wave-function is achieved by isolating the sideband with a filter function, such as a von Hann window, translation to zero-frequency, and then an inverse Fourier transform is applied. The Hann window has historically often been referred to as the 'Hanning' window, in confusion with the similar but different Hamming window.

To introduce the spatial frequency dependence, the electron counts is defined as [20],

$$\mu = t_x I_e R \times DQE_{ccd}(\mathbf{q}) \tag{3}$$

where $\mathbf{q} = q_x \hat{\mathbf{x}} + q_y \hat{\mathbf{y}}$, is the spatial frequency coordinate, t_x is exposure time, I_e is the electron flux at the object plane, and R is the rescale factor of the Fourier filter window. The effective dose is reduced by the detector quantum efficiency (DQE) [26]. We use a simplified version of the DQE_{ccd}(\mathbf{q}) = MTF²_{ccd}(\mathbf{q})/NTF²_{ccd}(\mathbf{q}), where MTF_{ccd} is the holographic MTF and NTF_{ccd} is the noise-transfer function [24]. This is not a complete treatment of the DQE as it does not account for the variation in DQE with dose, but it does effectively estimate the increase in shot noise over the expected Poisson value.

The factor R appears due to the downsampling that occurs in Fourier-space by the filter window in the reconstruction process [27,28]. For a circular hard-style window (which is zero outside the radius *a*), such as the von Hann window used throughout this paper, we find that

$$R = (2\sqrt{2}/a)^2$$

where a is the radius of the von Hann window (in reciprocal space units). The additional factor of $\sqrt{2}$ is the Ishizuka resampling factor, due to the shape mis-match between the square detector and rotationally-symmetric filter window [27,28].

In general, the filter radius a is chosen to be some fraction of the carrier frequency $q_c = xa$. The value of x chosen depends on the assumptions made regarding the nature of the specimen. As x increases, the low-pass filter becomes tighter and as a result spatial resolution is lost but nominally more shot noise is removed from the reconstruction. In practice the amount of shot noise removed depends on the power spectral density of the hologram relative to the distribution of the shot noise.

For strongly scattering objects historically x=3 has been popular due to the assumption that the centerband has twice the bandwidth of the sideband for a strongly-scattering specimen [29]. The historical justification for choice of bandwidth was due to uncertainty associated with the optical reconstruction process and non-linearity of the film emulsions used to record the hologram. In contrast Izhisuka showed that for a weak-phase object the filter radius can essentially be $a=q_c$ [27].

In practice for digital holographic reconstruction the experimental roll-off can be computed from the rotational average of the sideband and centerband magnitude. The average bandwidth for the 150-hologram series discussed in Section 4 is shown in Fig. 1. In signal-processing the roll-off radius r_{ro} for a filter can be expressed as the $-10\,\mathrm{dB}$ level (where the signal amplitude is 31.6% of the maximum value). The roll-off radius, computed by bilinear interpolation, of the centerband is $0.033\,\mathrm{nm}^{-1}$ and the sideband is $0.084\,\mathrm{nm}^{-1}$, as compared to the carrier frequency of $6.34\,\mathrm{nm}^{-1}$. For the reference hologram, the roll-off radius of the

Download English Version:

https://daneshyari.com/en/article/1677434

Download Persian Version:

https://daneshyari.com/article/1677434

<u>Daneshyari.com</u>